

See discussions, stats, and author profiles for this publication at: <https://www.researchgate.net/publication/266944501>

In Situ Observation of Water Behavior at the Surface and Buried Interface of a Low-K Dielectric Film

ARTICLE in ACS APPLIED MATERIALS & INTERFACES · OCTOBER 2014

Impact Factor: 6.72 · DOI: 10.1021/am504833v · Source: PubMed

CITATIONS

5

READS

33

5 AUTHORS, INCLUDING:



Xiaoxian Zhang

National Center for Nanoscience and Technol...

40 PUBLICATIONS 334 CITATIONS

[SEE PROFILE](#)



John Myers

University of Michigan

16 PUBLICATIONS 57 CITATIONS

[SEE PROFILE](#)



Qinghuang Lin

IBM

101 PUBLICATIONS 708 CITATIONS

[SEE PROFILE](#)

In Situ Observation of Water Behavior at the Surface and Buried Interface of a Low-K Dielectric Film

Xiaoxian Zhang,^{†,||} John N. Myers,^{†,||} Jeffery D. Bielefeld,[‡] Qinghuang Lin,[§] and Zhan Chen^{*,†}

[†]Department of Chemistry, University of Michigan, 930 North University Avenue, Ann Arbor, Michigan 48109, United States

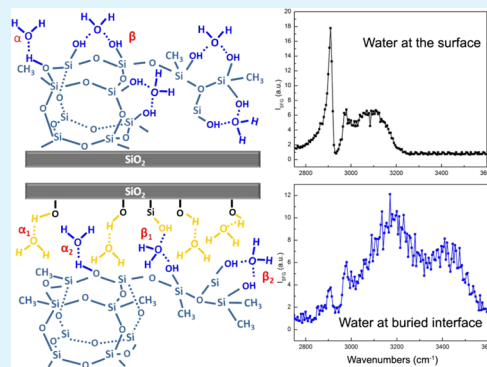
[‡]Intel Corporation, 5200 NE Elam Young Parkway, Hillsboro, Oregon 97124, United States

[§]IBM T. J. Watson Research Center, 1101 Kitchawan Road, Yorktown Heights, New York 10598, United States

Supporting Information

ABSTRACT: Water adsorption in porous low-k dielectrics has become a significant challenge for both back-end-of-line integration and reliability. A simple method is proposed here to achieve in situ observation of water structure and water-induced structure changes at the poly(methyl silsesquioxane) (PMSQ) surface and the PMSQ/solid buried interface at the molecular level by combining sum frequency generation (SFG) vibrational spectroscopic and Fourier transform infrared (FTIR) spectroscopic studies. First, in situ SFG investigations of water uptake were performed to provide direct evidence that water diffuses predominantly along the PMSQ/solid interface rather than through the bulk. Furthermore, SFG experiments were conducted at the PMSQ/water interface to simulate water behavior at the pore inner surfaces for porous low-k materials. Water molecules were found to form strong hydrogen bonds at the PMSQ surface, while weak hydrogen bonding was observed in the bulk. However, both strongly and weakly hydrogen bonded water components were detected at the PMSQ/SiO₂ buried interface. This suggests that the water structures at PMSQ/solid buried interfaces are also affected by the nature of solid substrate. Moreover, the orientation of the Si-CH₃ groups at the buried interface was permanently changed by water adsorption, which might due to low flexibility of Si-CH₃ groups at the buried interface. In brief, this study provides direct evidence that water molecules tend to strongly bond (chemisorbed) with low-k dielectric at pore inner surfaces and at the low-k/solid interface of porous low-k dielectrics. Therefore, water components at the surfaces, rather than the bulk, are likely more responsible for chemisorbed water related degradation of the interconnection layer. Although the method developed here was based on a model system study, we believe it should be applicable to a wide variety of low-k materials.

KEYWORDS: low-k material, molecular structure, water component, interface, vibrational spectroscopy, sum frequency generation



INTRODUCTION

Low-k materials and copper have been introduced to replace silicon dioxide and aluminum as interconnections in high performance integrated circuits to improve resistance-capacitance (RC) delay, minimize crosstalk-noise, enhance signal transmission, and reduce power dissipation.^{1–3} SiCOH based porous low-k dielectric materials have been studied extensively as intrametal dielectrics in recent years.³ Especially, silsesquioxane (SSQ) materials have a silica-like structure but with a fraction of the Si-O bonds replaced with other bonds, which have lower polarizability such as Si-CH₃, Si-C, and Si-F. The most common replacement is Si-CH₃ and the resultant materials are called methylsilsesquioxane (MSQ). Disruption of the silica structure with such groups increases the hydrophobicity of the resultant low-k material and reduces the relative dielectric constant to as low as 2.8.³ Cage structures as well as nanopores were additionally introduced into the materials to further lower the overall dielectric constant to below 2.8, depending on the porosity of SSQ film.^{1,4}

The integration of porous low-k dielectrics into large-scale microelectronic circuits, however, has been found to be extremely challenging. The introduction of high porosity has been reported to degrade the mechanical properties and thermal stability of the materials as compared with SiO₂.^{2,5,6} For instance, the poor mechanical strength of porous low-k dielectric films induced higher interfacial delamination and cohesive failure during chemical mechanical polish (CMP).⁷ In addition, high porosity has been related to increased diffusion rates of molecular species and metal ions into low-k bulk and weaker dielectric breakdown strengths relative to SiO₂.

For porous dielectrics, there are additional concerns related to moisture uptake induced by processing steps such as resist removal, postetch cleaning, CMP, or post-CMP cleaning.^{8–10} Previous reports showed that moisture could diffuse into the

Received: July 22, 2014

Accepted: October 14, 2014

Published: October 14, 2014



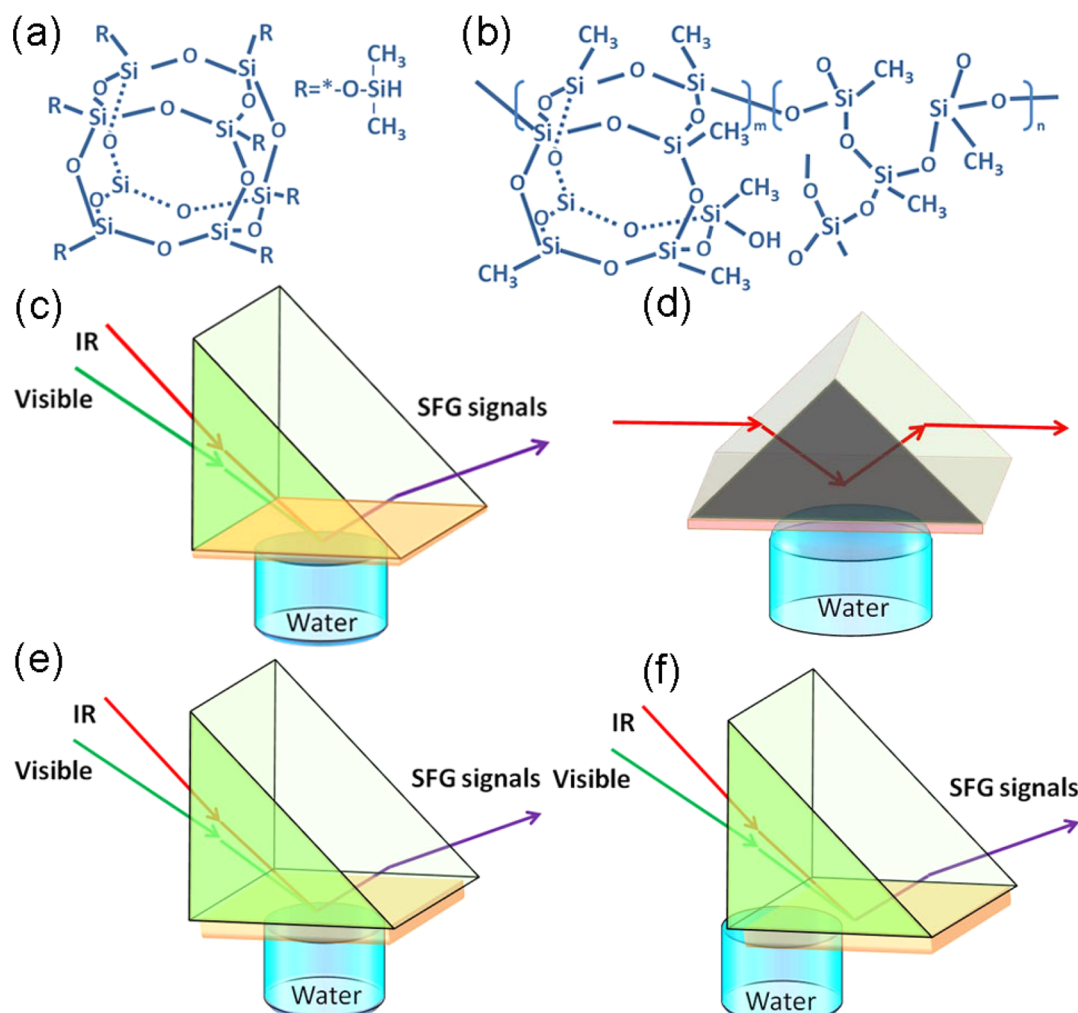


Figure 1. Chemical structures of monomer (a) PSS and (b) PMSQ. Experimental geometry of SFG experiment with a PMSQ thin film in contact with water (c), ATR-FTIR experiment with a PMSQ thick film in contact with water (d), SFG experiment with water in contact with PMSQ thick film at the middle of the film (method 1) (e) and at the edge of the film (method 2) (f).

SSQ film stacks even though SSQ materials are usually hydrophobic.¹¹ Water uptake is detrimental to the performance and the reliability of integrated circuits. Increased water in the low-k materials can lead to significantly increased leakage current, lower breakdown electric fields, and shorter dielectric breakdown lifetimes because water could increase dielectric permittivity, accelerate fracture behavior, and degrade the adhesion between the low-k material and the capping layer.⁸

Recently, extensive research has been carried out to understand the impact of water on the properties and the reliability of low-k materials.^{9,10,12,13} Many techniques, such as Fourier transform infrared (FTIR) spectroscopy, Raman vibrational spectroscopy, and thermal desorption spectroscopy (TDS) have been widely implemented to evaluate the influence of absorbed water on the low-k dielectric reliability and the bulk molecular structure of low-k materials.^{4,12,14} For example, Li et al. suggested that there was more than one kind of possible water components in the low-k dielectric.⁹ Physisorbed water could be easily removed by a low-temperature anneal which improved leakage current and time-dependent-dielectric-breakdown (TDDB) lifetime. Another type of water, referred to as chemisorbed, however, was only able to be desorbed after annealing at temperatures as high as 400 °C and was thus

thought to be the main reason for water related TDDB failure mechanism.⁹ Nevertheless, there is still a lack of a direct measurement technique to reveal the dynamic moisture uptake process and the water adsorption mechanism at the molecular level. In particular, few studies have been done to elucidate the influence of different absorbed water components at the surface and the interface of low-k dielectrics on device performance.

Surfaces and buried interfaces play an increasingly important role as the porosity of low-k dielectrics increases and the size of the microelectronic devices continues to shrink. In the past few decades, both theoretical and experimental results have shown that water molecules at surfaces could behave differently than in the bulk.¹⁵⁻²² Previous simulation results indicated that for certain low-k materials, ~0.4 vol % chemisorbed moisture found on the pore surface could induce a 17–23% increase of the dielectric constant.²³ Water diffusion along the interface of a low-k material has been observed experimentally with isotope tracer diffusion experiments combined with dynamic secondary ion mass spectroscopy (SIMS);⁸ however, no molecular structural information about interfacial adsorbed water could be obtained. More importantly, the water uptake process may be influenced by high vacuum environments needed for conducting the analysis. For a porous low-k material, moreover,

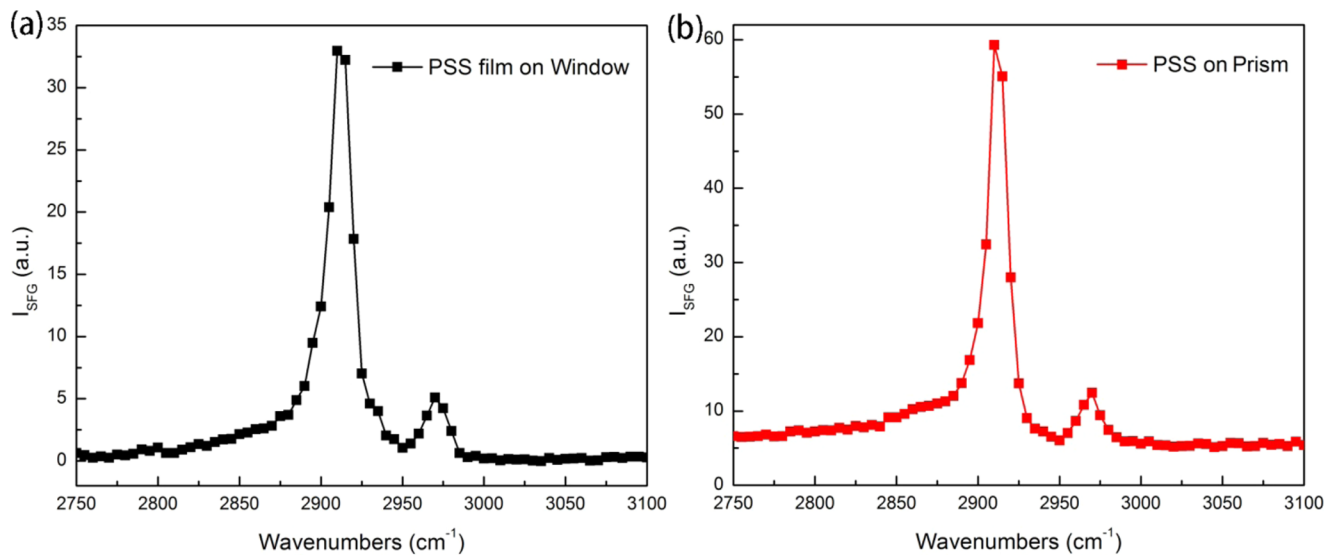


Figure 2. ssp SFG spectra of PSS on fused silica window (a) and prism (b).

the inner surfaces of the pores form another important interface, which is challenging to characterize. For a low-k material with a high porosity, the total area of these low-k material/air surfaces could be much larger than that of the low-k/solid interface. Therefore, water adsorption at these low-k material/air surfaces cannot be ignored and these surfaces increasingly influence the film properties and reliability as the porosity of low-k film increases. The introduction of higher porosity into low-k dielectric is required in the near future to further lower the dielectric constant.

Herein, to address the problems above, we propose a simple and direct method using sum frequency generation vibrational spectroscopy (SFG), transmission FTIR, and attenuated total reflectance FTIR (ATR-FTIR) to investigate water behavior at the exposed surface and buried interface of low-k dielectrics as well as probe the dynamic water uptake process through low-k material in situ at the molecular level. SFG is a second order nonlinear optical technique that can selectively and non-destructively probe the molecular structures of polymers^{24,25} and biomolecules²⁶ at surfaces and buried interface in situ with high surface selectivity due to its selection rules.^{27–39} Here, water behavior at the low-k dielectric/air surface was first investigated at the molecular level to simulate water adsorption at the pore inner surfaces of porous low-k dielectrics. Subsequently, combining SFG, transmission FTIR, and ATR-FTIR, the water uptake was selectively investigated to trace preferential water uptake pathways directly. Various water molecular structures were compared at the low k material/SiO₂ buried interface and in the bulk to correlate the molecular structure changes to low-k properties. To emulate the molecular structures of low-k materials, we selected a caged SSQ and poly(methylsilsesquioxane) (PMSQ) as model low-k materials.

MATERIALS AND METHODS

Materials. PSS-Octakis (dimethylsilyloxy) substituted (PSS) was purchased from Sigma-Aldrich (St. Louis, Mo) and poly(methyl silsesquioxane) (PMSQ) ($\geq 99.5\%$ purity) was purchased from Gelest. Tetrahydrofuran (THF; $\geq 99.9\%$ purity) was obtained from Sigma-Aldrich (St. Louis, Mo) and used as received. Right angle fused silica prism substrates were obtained from Altos Photonics, Inc.

Sample Preparation. Both PSS and PMSQ were dissolved in THF to form 2 wt % solutions. Then, PSS and PMSQ thin films were prepared on silica windows by spin coating (3000 r/min, 30 s) using a P-6000 spin coater (Speedline Technologies). Drop-casting was used to prepare PMSQ thick film for buried interface investigation. Similar drop-cast thick films were deposited on Si prism for ATR-FTIR measurements. The samples were then placed in a vacuum chamber (200 mTorr) for about 12 h at room temperature to completely evaporate residual solvent. Notably, since almost no SFG signals were detected using a face-down window geometry when samples were in contact with water, fused silica prisms were also applied here to provide in situ surface structure information on PMSQ thin films in contact with water.^{27–29,40} Film thicknesses were measured by a depth profilometer (Dektak 6 M Stylus Surface Profilometer, Veeco) and the average thicknesses of thin films and thick films were around 200 nm and 5 μm , respectively.

SFG and FTIR Experimental. The SFG setup used in this research was a commercially available system purchased from EKSPLA. The optical setup has been reported in detail previously.^{27–30,32} The SFG spectra were collected in the ssp (s-polarized signal output, s-polarized visible input, and p-polarized IR input) polarization combination. All SFG spectra collected here were measured by using the face-down reflection geometry (Figure 1c, e, f). For each sample, spectra were collected at least at five different spots; for each spot, five spectra were detected to examine the film homogeneity. FTIR and ATR-FTIR measurements were performed using a Nicolet 6700 FTIR spectrometer controlled by OMNIC software. The experimental setup for ATR-FTIR tests during water uptake process is illustrated in Figure 1d. The input angle was approximately 55°.

RESULTS AND DISCUSSION

1. SFG Study of the PSS Thin Film. First, PSS with high purity was selected as a simple model system for peak assignments. As shown in Figure 1a, PSS has a cage structure containing 8 silicon atoms and substituent R. Here, R, whose structure is shown in Figure 1a, contains Si-CH₃ and Si-H groups. The chemical structure of PSS is very similar to the widely used low-k material PMSQ and poly(hydrosilsesquioxane) (HSQ). Figure 2 shows ssp SFG spectra collected from a spin-coated PSS thin film on a silica window and a prism, respectively. Two pronounced peaks were observed near 2915 and 2970 cm^{-1} , which can be assigned to Si-CH₃ symmetric and asymmetric stretching modes, respectively (Figure 2a).⁴¹ The intensity of the symmetric stretching

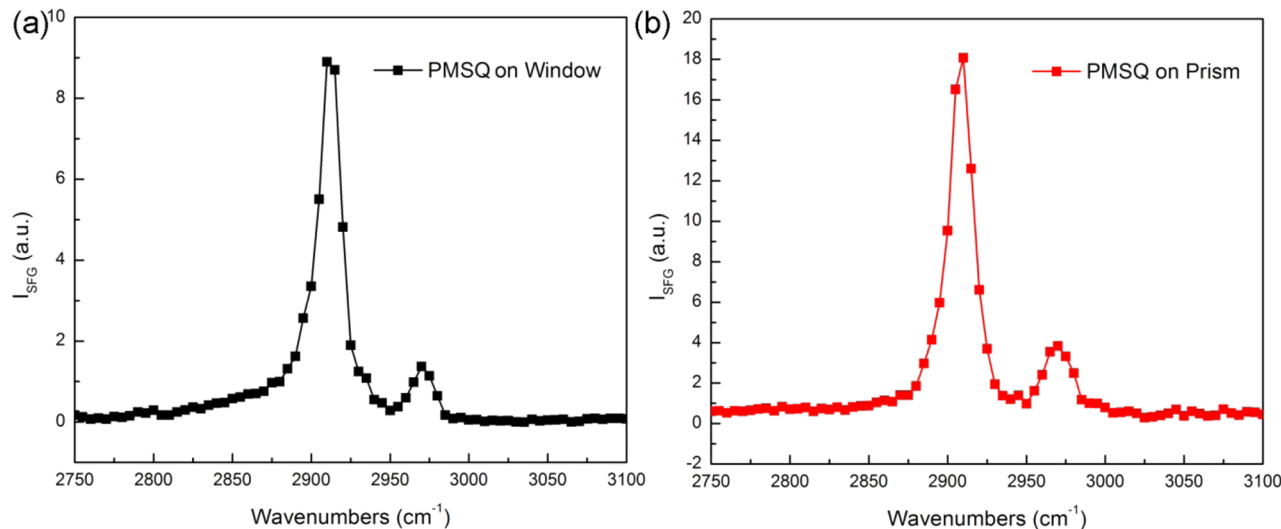


Figure 3. ssp SFG spectra of PMSQ on fused silica window (a) and prism (b).

signal was much stronger than that of the asymmetric stretching peak. According to a previous study,⁴² for windows geometry, SFG signals in the C–H stretching frequency region from the polymer/hydrophilic substrate are usually quite weak, so ssp SFG spectrum collected from windows face-down geometry can be considered to be dominated by the SFG signals generated from polymer/air surface. Therefore, the SFG spectrum shown in Figure 2a indicates that Si–CH₃ functional groups cover the surface of the PSS film. Figure 2b exhibits the ssp SFG spectra collected from the PSS thin film coated on silica prism. Not surprisingly, very similar spectral features were observed around 2915 and 2970 cm⁻¹ with a similar intensity ratio relative to the window geometry, which suggests that ssp SFG spectrum of PSS thin film using prism geometry can be considered to be dominated by PSS/air surface signals as well. The only difference is the peak intensities are substantially higher than those collected with window geometry, which is reasonable because prism geometry has been shown to enhance SFG intensities.⁴³

2. SFG and FTIR Studies of the PMSQ Thin Film in Air.

After using PSS to assign the peaks in ssp SFG spectra, SFG measurements were carried out on PMSQ thin film spin-coated on a silica window (Figure 3a) and prism (Figure 3b) as well. The molecular structure of PMSQ is shown in Figure 1b. Different from the monomer PSS, PMSQ consists of two kinds of Si–O structures, which are often referred to as “cage” and “network” structures. In addition to Si–O bonds, Si–CH₃ functional groups are also present in the PMSQ structure. Similar to the case of PSS, the ssp SFG spectrum collected from the PMSQ thin film using window geometry was dominated by two peaks near 2915 and 2970 cm⁻¹, indicating that the surface of PMSQ thin film is covered by Si–CH₃ groups as well. Despite the similar spectral features of PSS and PMSQ, the asymmetric peak (2970 cm⁻¹) strength is higher here, leading to slightly different orientation of Si–CH₃ groups at the surface of PMSQ film compared to the PSS film. Besides, the peak intensities observed in Figure 3a are lower than that of the PSS thin film, which could be interpreted by a less ordered surface or less coverage of Si–CH₃ groups at the surface of the PMSQ film. Considering the similar molecular structures of PSS and PMSQ, we believe the surface of PMSQ thin film was more disordered than that of PSS.

Similar SFG spectral features were again observed in the prism and window geometry (Figure 3b) for PMSQ thin films. As in the PSS case, the SFG intensity was enhanced in the prism geometry. However, the peak intensities detected here are still lower than that of the PSS film, implying less ordered surface of PMSQ compared to that of PSS. As expected, two pronounced peaks, 2915 and 2970 cm⁻¹, with similar peak ratio as the two peaks in the SFG spectra collected from PSS films, were observed in the ssp SFG spectrum of PMSQ thin film. These results imply that the molecular structures at the surfaces of PMSQ films deposited on window and prism resembled each other, both of which are covered by Si–CH₃ groups with similar orientations. As the SFG spectral features of PMSQ thin films collected using silica window and prism are very similar, the prism geometry was utilized below for water contact experiments.

To clarify the impact of the interference of SFG signals originating from the buried interface and the surface, the Fresnel coefficients in the PMSQ/silica buried interface and PMSQ/Medium (air/water) were calculated using a thin film model,⁴² and the corresponding calculated Fresnel coefficients were plotted as a function of film thickness (shown in Supporting Information Figure S1). Besides, PMSQ thin films were spin-coated on the surfaces of silica windows and prism with different thicknesses to clarify that the origins of the ssp SFG signals collected from the PMSQ film using face-down window and prism geometry. The thickness dependent SFG spectra of PMSQ films deposited on fused silica windows and prisms were shown in Supporting Information Figure S2a and b, respectively (Supporting Information). A detailed discussion about the contribution of SFG signals using prism face-down geometry is shown in Supporting Information. Since the SFG signals were not influenced as the thicknesses of PMSQ films varied for both windows and prism geometry, we believe that the ssp SFG spectrum of PMSQ thin film is dominated by the SFG signals generated from polymer/air surface. Signals from polymer/substrate buried interface were proved to be extremely weak and should be able to be ignored in this paper.

To compare the chemical structures of PMSQ bulk to that of PMSQ surface, FTIR measurement was performed on as-deposited PMSQ thin film to characterize the bulk structure. With regard to possible water components in low-k materials,

Proost et al. reported that there may exist four types of water related chemical groups, which were attached to the skeleton for silica based dielectrics.^{12,44} Li et al. pointed out that two of them, physisorbed (α) and chemisorbed (β) water, were found to degrade the dielectric reliability of integrated low-k materials and selective studies have elucidated the respective contributions of α water and β water to increased leakage current and TDDB failure.⁹ The other two kinds of water present in low-k dielectrics, γ_1 and γ_2 , were not able to be desorbed by conventional anneal, which is compatible with low-k materials unless the anneal temperature was as high as 700 °C. As a result, only the first two kinds of water will be considered for the water adsorption mechanism and the influence of different kinds of adsorbed water on low-k properties here. Figure 4

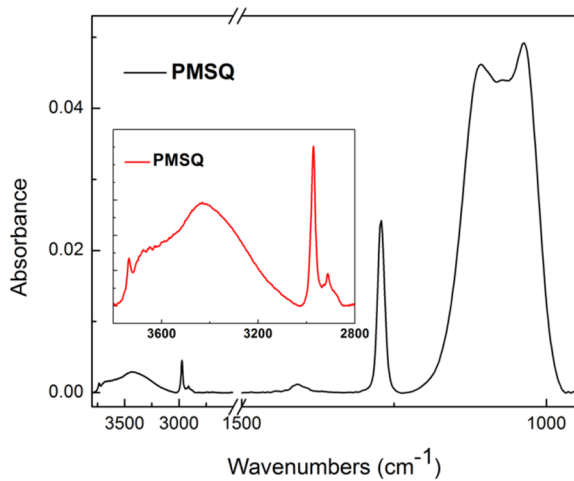


Figure 4. Transmission FTIR spectrum of PMSQ thin film spin coated in CaF_2 window, the inset is the enlarged spectrum in C–H and water region.

shows that the FTIR spectral features are very similar to most carbon-doped oxide low-k films.^{1,4,13} In the fingerprint region, several clear peaks were observed. The peak around 1272 cm^{-1} can be assigned to $\text{Si}-\text{CH}_3$ and the two strong overlapped peaks around 1109 and 1035 cm^{-1} can be assigned to caged $\text{Si}-\text{O}$ bond structure and network $\text{Si}-\text{O}$ bond structure, respectively.⁴ In the C–H stretching frequency region, only one weak CH_3 peak near 2971 cm^{-1} and a strong water peak from 2975 to 3800 cm^{-1} centered around 3400 cm^{-1} were detected. Such FTIR features have been attributed to weakly hydrogen bonded water located inside the PMSQ bulk, which suggests that most of the water molecules (e.g., those that contribute to the signal centered at 3400 cm^{-1}) present in PMSQ bulk (Figure 4) should be removed after annealing above 100 °C. However, the broad peak feature ranging from 2975 to 3800 cm^{-1} implies that a small part of other water components, such as those with peak centered near 3200 cm^{-1} may also be present in the PMSQ bulk. This peak has been assigned to strongly hydrogen bonded water (e.g., those with strong hydrogen bonding interactions with hydrophilic sites within a polymer; they were called chemisorbed water).^{12,45} According to a previous study,²³ only a small amount of this type of water molecules exist in low-k materials. The previous FTIR characterization of the PMSQ bulk structure is consistent with this result. Note that after curing the PMSQ film under vacuum at 400 °C for 1 h, the water peak became almost undetectable by FTIR.²³

3. Water Uptake at the Surface and Buried Interface of PMSQ Film.

In order to reveal the water behavior at the PMSQ surface and correlate the water structures to low-k degradation, in situ SFG measurements were first performed on a spin-on PMSQ thin film deposited on silica prism. SFG studies on the surface of PMSQ thin film during contact with water and after water removal were subsequently performed.

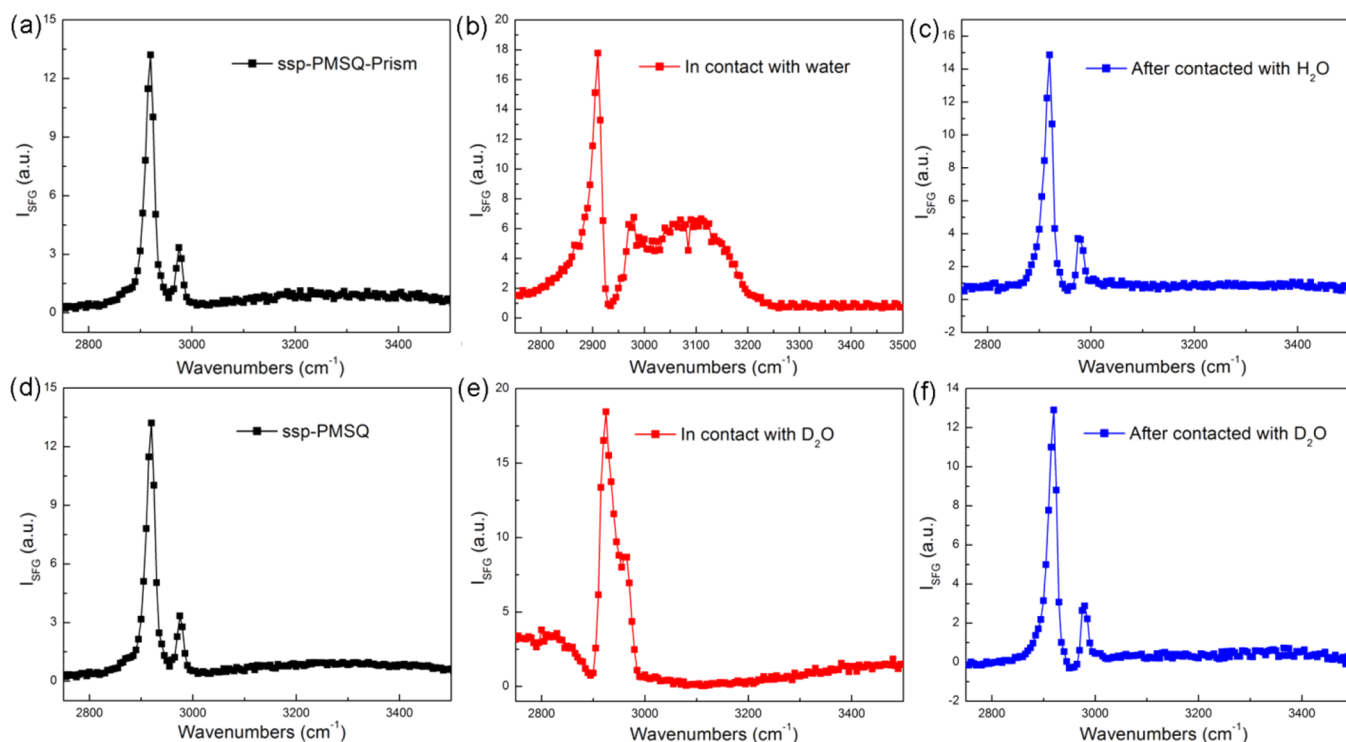


Figure 5. ssp SFG spectra collected from the PMSQ surface before, during, and after contacting with H_2O (a–c) and D_2O (d–f).

The experimental setup for in situ SFG investigation of PMSQ surface structures in contact with water was depicted in Figure 1c. To selectively detect the molecular structural changes in the C–H stretching frequency region, D₂O was applied in SFG experiments to remove the influence of H₂O on SFG signals in the C–H region. Figure 5 shows the ssp SFG spectra collected from the PMSQ surface before, during, and after water contact (Figure 5a–c). D₂O results are also shown in Figure 5d–f.

Figure 5a shows the original ssp SFG spectra of PMSQ thin film in the C–H and water O–H stretching frequency region (2750 cm⁻¹ to 3500 cm⁻¹). Except for pronounced Si-CH₃ signals, no water peaks were detected, indicating that no ordered water structures were present at the PMSQ/air surface. It is interesting to see that water behaved very differently at the PMSQ surface than in the bulk (a broad water peak around 3400 cm⁻¹ was detected by FTIR). Once the film was in contact with water, a broad water peak centered near 3150 cm⁻¹ was observed in the SFG spectrum (Figure 5b). This means although PMSQ is quite hydrophobic, ordered water components can be present at the PMSQ/water interface. The water peak near 3200 cm⁻¹ has been assigned to strongly hydrogen bonded water.^{12,19,20} The presence of an SFG feature centered near 3150 cm⁻¹, which is shifted from the 3200 cm⁻¹ peak to a lower wavenumber, suggests the formation of strong hydrogen bonded water at the PMSQ/water interface. Combining FTIR and SFG results above (Figure 4 and Figure 5), we can conclude that water tends to form strong hydrogen bonding with PMSQ (~3150 cm⁻¹) at the PMSQ/water interface (evidenced by the SFG result). Whereas water molecules are more flexible in the bulk, that is, they prefer to stay in the bulk by forming weak hydrogen bonds (evidenced by FTIR result). Moreover, the intensity of the SFG water peak did not change much while contacting with water for a longer time, showing that formation of strongly hydrogen bonded water at the PMSQ surface is quite fast.

According to the previous studies, the chemisorbed water components are more difficult to be removed from the low-k network than physisorbed water.^{9,12} However, detection of such water components at the pore inner surfaces is quite challenging because the amount of these water components is small. Here, we employed SFG measurements with high surface sensitivity to obtain direct evidence of chemisorption as water molecules reached the PMSQ surface. It is suggested that when water molecules reach the pore inner surfaces of porous low-k materials, they tend to form strong hydrogen bonds with the low-k material at the pore inner surfaces. Since these chemisorbed water components have been closely related to the TDDB failure mechanism of low-k materials,⁹ we believe that the chemisorbed water molecules at the pore inner surfaces are mainly responsible for these negative effects on low-k material properties than the water components in the bulk (e.g., those inside the pores but not interacting with the pore surfaces).

SFG signals in the C–H stretching frequency region were enhanced during contact with water. Considering the Fresnel coefficient change from the polymer/air surface to the polymer/water interface,⁴² the normalized peak intensity of the methyl peaks (Figure 5b) should be higher. Compared to the peak in air (Figure 5a), the intensity of the symmetric Si-CH₃ stretch is slightly higher compared to the peak in air, indicating that Si-CH₃ groups were slightly more ordered at the PMSQ/water interface when water molecules formed strong hydrogen bonds with PMSQ. We speculate that the ordering of

Si-CH₃ groups at the surface during contact with water is likely related closely to the formation of strong hydrogen bonds between water and PMSQ at the PMSQ surface. Therefore, the intermediate intensity of the water peak in Figure 5b should be attributed to the small amounts of ordered water components at the PMSQ surface rather than less ordering of water molecules. Additionally, after removing the PMSQ film from water, the surface of PMSQ thin film was found to dry immediately and the molecular structure was also observed to recover to its original structure before water contact (Figure 5c). That is, no water peaks were observed at surface by SFG after drying, which could be ascribed to no ordered water components or no water molecules left at the surface. Considering the difficulty of breaking these strongly hydrogen bonds, it is most likely that ordered water structures formed at PMSQ surface under water environment become disordered in air.

To avoid the influence of the water peak at 2900–3000 cm⁻¹ in the C–H stretching frequency region, D₂O was also utilized to clarify the molecular structure changes of the PMSQ surface in contact with water. Parts e and f of Figure 5 show the ssp SFG spectra collected from the PMSQ/D₂O interface and the PMSQ/air surface after removal of D₂O, respectively. Similar to the observation when PMSQ was in contact with H₂O, stronger Si-CH₃ peaks around 2915 and 2970 cm⁻¹ were detected during contacting with D₂O. The stronger intensities here suggest that Si-CH₃ groups become more ordered at the PMSQ surface during water contact. After removing D₂O, the SFG spectrum closely resembled the original one shown in Figure 5a. This implies that surface molecular structures were recovered after removing water. Therefore, the molecular structure of PMSQ at pore inner surfaces will not be permanently influenced by water for porous low-k material.

SFG spectra were also collected from a cured PMSQ thin film before, during, and after contact with water and D₂O (shown in Supporting Information Figure S3). The surface structures were found to be almost unchanged after curing at 400 °C for 1 h. However, during contact with water, water signals at the cured PMSQ surface were much stronger than those in spectra collected from the uncured film. A strong peak around 3150 cm⁻¹ (chemisorbed water component) and a relatively weak peak near 3400 cm⁻¹ (physisorbed water component) were detected in the SFG spectrum (Supporting Information Figure S3b). According to previous studies, low-k material may be slightly more hydrophilic after curing because a portion of the C–H components might be removed during the curing process.⁴ We believe the increased hydrophilicity after curing should be responsible for the enhancement of water signals at the cured PMSQ surface. Moreover, the D₂O experiments shown in Supporting Information Figure S3d and e demonstrate that Si-CH₃ signals also become much higher during contact with D₂O. This trend is very consistent with the uncured results. Additionally, these results also support our hypothesis that the ordering of Si-CH₃ groups should be driven by the formation of strongly hydrogen bonded water at the PMSQ surface. These SFG observations on cured samples also demonstrate that the method developed here is general and can be applied to investigate the water behavior at low-k material interfaces after various treatments.

Subsequently, the water uptake process through PMSQ bulk or PMSQ/substrate buried interface was selectively investigated in situ by SFG measurements. Two contrast experiments were designed to directly trace the preferential pathway of water

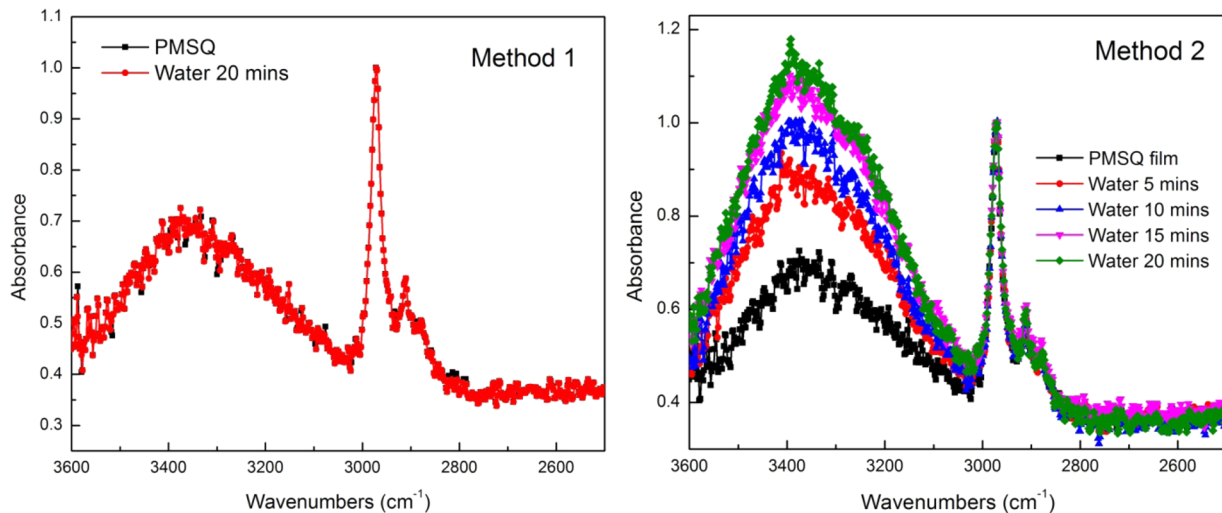


Figure 6. Series of ATR-FTIR spectra collected from PMSQ in contact with H_2O as a function of time (a) using “method 1” shown in Figure 1e and b “method 2” shown in Figure 1f.

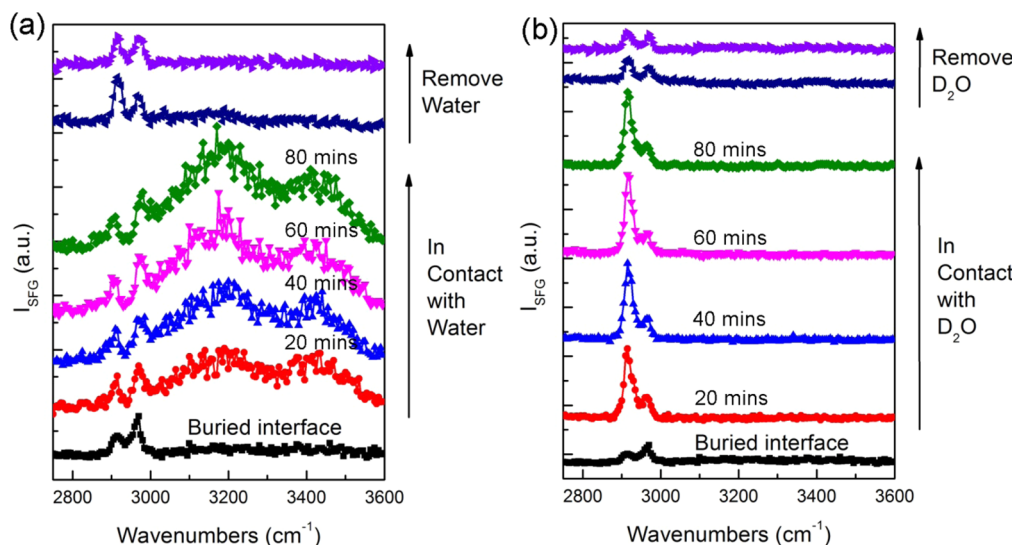


Figure 7. Series of ssp SFG spectra collected from the PMSQ/ SiO_2 buried interface before and during contact with H_2O (a) and D_2O (b) as a function of time and then after water removal using “method 2” (Figure 1f).

uptake via combined FTIR and SFG measurements. Drop-cast PMSQ thick films were utilized here to block SFG signals from the PMSQ surface. The experimental setups for these two experiments are schematically illustrated in Figure 1e and f. At first, a water drop was placed in contact with the surface of the PMSQ thick film. Subsequently, in situ SFG and ATR-FTIR measurements were performed on and near the PMSQ/ SiO_2 buried interface respectively to detect the changes of water signals. If water signals were found to gradually increase, the water uptake primarily occurred through the PMSQ bulk; we name this method as “method 1” (Figure 1e). As a contrast, as a water drop was placed in contact with the edge of the PMSQ thick film, SFG and ATR-FTIR measurements were conducted at the center of the thick film, so increased water signals would indicate water uptake along the buried interface (Figure 1f). We name this method as “method 2”. Since the film thickness was around $5.0 \mu\text{m}$, while the distance from film edge to film center was around 0.5 cm , it should be possible to trace the preferential water uptake pathway by comparing the water

signals in ATR-FTIR and SFG spectra using “method 1” and “method 2”.

In-situ ATR-FTIR measurements were implemented on PMSQ thick films drop-casted on Si prisms using “method 1” and “method 2”, separately. Similar to the FTIR spectrum of PMSQ film shown in Figure 4, the original spectrum of PMSQ thick film detected by ATR-FTIR was dominated by a C–H stretching peak around 2970 cm^{-1} as well as a broad water O–H stretching peak centered at $\sim 3390 \text{ cm}^{-1}$. It is noticeable that the water peak center is slightly blue-shifted, which could be due to a higher contribution of the chemisorbed water component near $\sim 3200 \text{ cm}^{-1}$ to the broad water peak at the buried interface. The ATR-FTIR penetration depth was approximately 500 nm , so the water peak characterizes molecular structure 500 nm near the PMSQ buried interface. However, following “method 1”, no detectable increase of water signals were found in ATR-FTIR spectra even after contact with water for 20 min (Figure 6a), indicating that water uptake through the hydrophobic PMSQ film is relatively slow. As a contrast, using “method 2”, the water peak around 3390 cm^{-1}

was observed to gradually increase after water contact. The rate became slower as time increased, which may be due to gradual saturation of water in the bulk near the buried interface. The corresponding ATR-FTIR spectra of PMSQ thick films were collected during contact with water after 5, 10, 15, and 20 min (shown in Figure 6b). The water signals were found to be unchanged after 20 min, which again may be due to the saturated water near the buried interface. These results indicate that water molecules transport through PMSQ/solid interface faster than through the bulk. These results are consistent with previous reports which utilized isotope-label tracer and SIMS.⁸ It is notable that the small shoulder near 3200 cm^{-1} was more evident in the ATR-FTIR spectrum after contact with water for 20 min, which might be attributed to the formation of strongly hydrogen bonded water near the PMSQ/SiO₂ buried interface.

In order to further elucidate water behavior at the PMSQ/SiO₂ buried interface and correlate the molecular structure to the degradation of low-k properties, corresponding SFG measurements using “method 1” and “method 2” were conducted on the drop-cast PMSQ thick films on fused silica prism. First, we can see from Figure 7a that the ssp SFG spectrum collected from the PMSQ/SiO₂ buried interface was dominated by two Si-CH₃ peaks around 2915 and 2970 cm⁻¹, respectively. However, the asymmetric stretching peak (2970 cm⁻¹) was stronger than the symmetric stretching peak (2915 cm⁻¹). This result indicates that although the PMSQ/SiO₂ buried interface is also dominated by Si-CH₃ groups, the orientation of Si-CH₃ groups at buried interface is different from that of surface.⁴⁶ The strong asymmetric peak suggests that Si-CH₃ groups were oriented more parallel to the substrate at the buried interface, whereas at the surface the groups tended to orient more perpendicular to the substrate. In addition, no water peaks were detected at the buried interface, indicating that no water molecules were present at the buried interface or that the water molecules were randomly oriented. After contact with water, using “method 1”, no water signals were detected by SFG from the PMSQ/SiO₂ buried interface after contact with water after 20 min, which suggests that no ordered water was present at the buried interface. This is in consistent with the corresponding ATR-FTIR results shown in Figure 6a. However, when using “method 2”, two water peaks around 3200 and 3400 cm⁻¹ appeared in SFG spectrum collected from the PMSQ/SiO₂ buried interface soon after contact with water. Different from the PMSQ surface, both chemisorbed (strongly hydrogen bonded) and physisorbed (weakly hydrogen bonded) water components formed at the PMSQ/SiO₂ buried interface. The possible mechanisms of various water behaviors at PMSQ surface and the PMSQ/SiO₂ buried interface will be discussed later. Here, we can see in Figure 7a that as the water contact time increased, these two water peaks continued to increase slowly. In particular, the intensity of 3200 cm⁻¹ peak increased more quickly than that of 3400 cm⁻¹ peak. Time-dependent SFG observations were also utilized to compare the kinetics of formation of these two water peaks at the buried interface during the water uptake process. The corresponding time-dependent SFG spectra and their fitting curves are shown in Figure S4 (Supporting Information) and the time-dependent fitting results of the two water components are shown in Supporting Information Table S1.

According to in situ ATR-FTIR observation of adsorbed water molecules shown above, water in the bulk near the buried interface would be saturated after 20 min. Since every SFG spectrum shown here took about 20 min to collect, it is

interesting to see that water signals, especially the water component located at $\sim 3200\text{ cm}^{-1}$ at the buried interface, still gradually increased even after contact with water for ~ 80 min. Supporting Information Figure S5 clearly exhibits the various rates of increase of the two water components. It is surprising to see that both of the water peaks quickly appeared after contact with water, indicating that water uptake through the buried interface is much quicker than through the PMSQ bulk. Different from the PMSQ surface in contact with water, the intensities of two peaks around 3200 and 3400 cm⁻¹ were both found to gradually increase and the rates of increase could both be fitted linearly after water arrived at the interface. This means that although relatively quick water uptake occurred through the PMSQ/SiO₂ buried interface, and the saturation of water molecules in the bulk near the buried interface occurred after 20 min, the formation of ordered water structures, especially strongly hydrogen bonded water, is a gradual process that continues to occur even after water saturation in the bulk near the buried interface. The spectral fitting results displayed in Supporting Information Table S1 indicate that the slope of 3200 cm⁻¹ curve is about twice as that of 3400 cm⁻¹ curve, which means chemisorbed water component near 3200 cm⁻¹ increases twice as quickly as that of 3400 cm⁻¹ peak at the PMSQ/SiO₂ buried interface after water reached the interface. The time-dependent results of the two water components shown in Supporting Information Figure S4 and Table S1 are consistent with the results exhibited in Figure 7a. We can also see from Figure 7a that the Si-CH₃ signals at the buried interface were also influenced by water, so D₂O experiments were performed to clarify the impact of water on the orientation of Si-CH₃ groups at the buried interface, which will be discussed in more details later.

Here, in addition to in situ observation of the water uptake process through the buried interface, Figure 7a also provides the ssp SFG spectra collected from the PMSQ/SiO₂ buried interface after water removal. Almost no water signals were detected immediately after removal of water from the PMSQ film surface; only a very small peak around 3200 cm⁻¹ was observed in the SFG spectra. This peak was undetectable after collecting the second SFG spectrum. Based on our previous discussion, we believe that the disappearance of water peaks in the SFG spectrum after removing water is due to disordering of these water components rather than the absence of water at the PMSQ interface in air after removing the sample from water. In addition, the ratio of two Si-CH₃ peaks was also affected by removal of water from the buried interface (Figure 7a). The symmetric stretching peak became dominant at the buried interface after water removal then the intensities of the symmetric and asymmetric stretching peaks were very similar. These results indicate that although no ordered water components were detected from the buried interface after water removal, the orientation of Si-CH₃ groups was permanently changed due to the formation of strongly hydrogen bonded water at the buried interface. This is very different from the PMSQ/air surface, which recovered when exposed to air again. According to the literature,^{9,12} in addition to the chemisorbed (β) and physisorbed (α) water molecules, there might be two other water components present in low-k materials, γ_1 (hydrogen-bonded to silanols) and γ_2 (hydrogen-bonded to isolated silanols). Annealing temperature as high as 700 °C has been recommended to remove these two water components. We therefore did not study these two types of water by high temperature annealing in this research and such

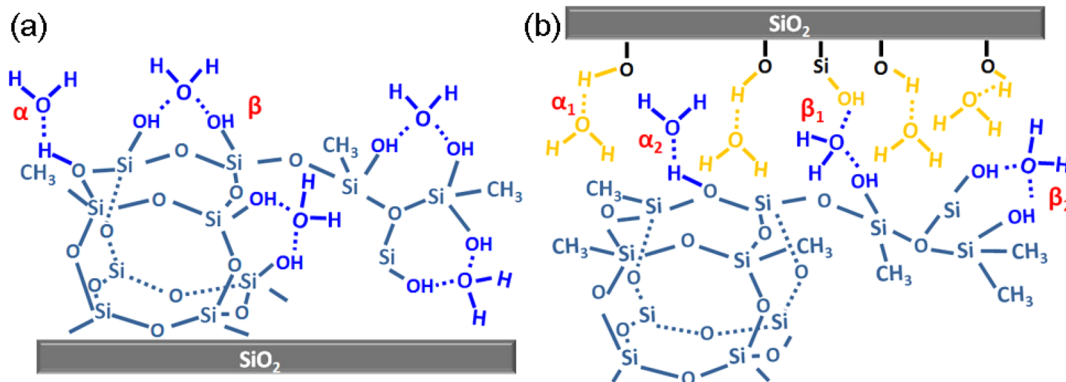


Figure 8. Schematic illustration of water structures at the PMSQ surface (a) and the buried interface (b) after water uptake.

high temperatures are not compatible with semiconductor interconnects. The permanent changes of the orientation of Si-CH₃ groups after water uptake at the buried interface might be due to the less flexibility of the functional groups at the buried interface than that at the PMSQ surface.

As mentioned before, D₂O experiments were also performed to clarify the molecular structural changes in the C-H stretching frequency region at the buried interface during contacting with water (Figure 7b). Similar to the H₂O case, strong Si-CH₃ signals were detected from the buried interface when the PMSQ thick film was in contact with D₂O. The enhanced peak intensities may be due to higher ordering or more coverage of reoriented Si-CH₃ groups at the PMSQ/SiO₂ buried interface. The symmetric Si-CH₃ peak (2915 cm⁻¹) was more pronounced than the asymmetric peak (2970 cm⁻¹), indicating that the Si-CH₃ groups at the buried interface tilted more toward the surface normal after water uptake. Just as we discussed before, we believe that the number of interfacial Si-CH₃ groups of PMSQ would not be changed due to water uptake, so the Si-CH₃ groups became more ordered as water molecules reached the buried interface and formed strong hydrogen bonds at the buried interface. Moreover, as the contact time increased, the peak intensities of symmetric and asymmetric Si-CH₃ peaks kept increasing with a relatively constant peak ratio. After removal of the D₂O, the SFG spectra collected from the PMSQ/SiO₂ buried interface were very similar to the H₂O results shown in Figure 7a.

Based on our *in situ* SFG and ATR-FTIR observations above, the possible water adsorption mechanisms at the PMSQ/water interface and PMSQ/SiO₂ buried interface are schematically illustrated in Figure 8. At the PMSQ/water surface, which resembles the inner surfaces of pores of low-k material, water tends to form strong hydrogen bonds (β) with PMSQ although there might still be some weakly bonded water elements (α) (shown in Figure 8a). At the PMSQ/SiO₂ buried interface (Figure 8b), water may also form hydrogen bonds with the SiO₂ substrate (α_1 and β_1 in Figure 8b).^{47,48} Considering the dominant β water observed in SFG spectrum collected from PMSQ/water surface, we believe the ordered water components attached to PMSQ at the buried interface should still be dominated by chemisorbed water (α_2 in Figure 8b) although both α_2 and β_2 should be present. It is suggested that these chemisorbed water components present at pore inner surfaces and at the buried interface are more responsible for the TDDDB failure in low-k dielectric reliability tests than the physisorbed water in the bulk.

CONCLUSION

In this study, a simple method was proposed and demonstrated to probe water molecular structures *in situ* at the PMSQ/water and PMSQ/substrate buried interfaces by combining SFG and FTIR measurements. First, selective *in situ* SFG observation of water uptake process provides direct evidence that water diffuses predominantly along the PMSQ/solid buried interface rather than through the porous low-k film and also that water uptake through the hydrophobic dense low-k film was slow. Moreover, *in situ* SFG measurements were conducted on the PMSQ/water interface to simulate water behavior at the pore inner surfaces for porous low-k materials. Most of the water molecules were found to be strongly bonded to the PMSQ surface. However, FTIR results showed that most of the water molecules were found to be weakly bonded to the bulk PMSQ. Meanwhile, Si-CH₃ groups at the PMSQ surface were observed to form ordered structures when water molecules were present, which may be driven by the formation of highly ordered water components at the surface. However, both strongly hydrogen bonded and weakly hydrogen bonded water were observed at the PMSQ/SiO₂ buried interface. Formation of both of these water components is influenced by the nature of the substrate. More importantly, the orientation of the Si-CH₃ groups at the buried interface was permanently changed due to water contact which might be due to the lower flexibility of Si-CH₃ groups at the buried interface. In brief, this study provide direct evidence that water molecules tend to form chemisorbed water components (strongly hydrogen bonded water) at two kinds of interfaces, that is, pore inner surfaces and low-k/solid interface of porous low-k materials, while weakly hydrogen bonded water components were detected in the bulk. Therefore, water at the surfaces, rather than the bulk, should be more responsible for TDDDB failure and chemisorbed water related degradation of the interconnection layer. Although the method developed here was based on the observation of a model system, we believe it should also be straightforward to analyze a wide variety of low-k materials.

ASSOCIATED CONTENT

S Supporting Information

Calculated Fresnel coefficients at the PMSQ/SiO₂ buried interface and PMSQ/medium surface (air or water), thickness dependent SFG spectra collected from the PMSQ thin films using both window face-down geometry and prism face-down geometry, SFG spectra collected from the cured PMSQ thin films, the time-dependent SFG water signals and the corresponding spectral fitting parameters, and a schematic

illustration of ordered Si-CH₃ groups at the PMSQ surface. This material is available free of charge via the Internet at <http://pubs.acs.org>.

AUTHOR INFORMATION

Corresponding Author

*Email: zhanc@umich.edu.

Author Contributions

[†]X.Z. and J.N.M. are co-first authors who equally contributed to this work.

Notes

The authors declare no competing financial interest.

ACKNOWLEDGMENTS

The authors thank Dr. Alfred Grill from IBM for useful discussion. This research is supported by Semiconductor Research Corporation (Contract No. 2012-KJ-2279).

REFERENCES

- (1) Grill, A. Porous Psicoh Ultralow-K Dielectrics for Chip Interconnects Prepared by PECVD. *Annu. Rev. Mater. Res.* **2009**, *39*, 49–69.
- (2) Shamiryan, D.; Abell, T.; Iacopi, F.; Maex, K. Low-k Dielectric Materials. *Mater. Today* **2004**, *7*, 34–39.
- (3) Maex, K.; Baklanov, M.; Shamiryan, D.; Brongersma, S.; Yanovitskaya, Z. Low Dielectric Constant Materials for Microelectronics. *J. Appl. Phys.* **2003**, *93*, 8793–8841.
- (4) Grill, A. Plasma Enhanced Chemical Vapor Deposited Sicoh Dielectrics: From Low-K to Extreme Low-K Interconnect Materials. *J. Appl. Phys.* **2003**, *93*, 1785–1790.
- (5) Li, Z.; Johnson, M. C.; Sun, M.; Ryan, E. T.; Earl, D. J.; Maichen, W.; Martin, J. I.; Li, S.; Lew, C. M.; Wang, J. Mechanical and Dielectric Properties of Pure-Silica-Zeolite Low-k Materials. *Angew. Chem., Int. Ed.* **2006**, *45*, 6329–6332.
- (6) Bao, J.; Shi, H.; Liu, J.; Huang, H.; Ho, P.; Goodner, M.; Moinpour, M.; Kloster, G. Mechanistic Study of Plasma Damage of Low K Dielectric Surfaces. *J. Vac. Sci. Technol., B* **2008**, *26*, 219–226.
- (7) Cheng, Y.-Y.; Kan, J. Y.; Lin, I. Adhesion Studies of Low-k Silsesquioxane. *Thin Solid Films* **2004**, *462*, 297–301.
- (8) Li, H.; Tsui, T. Y.; Vlassak, J. J. Water Diffusion and Fracture Behavior in Nanoporous Low-K Dielectric Film Stacks. *J. Appl. Phys.* **2009**, *106*, 033503.
- (9) Li, Y.; Ciofi, I.; Carbonell, L.; Heylen, N.; Van Aelst, J.; Baklanov, M. R.; Groeseneken, G.; Maex, K.; Tókei, Z. Influence of Absorbed Water Components on SIOCH Low-K Reliability. *J. Appl. Phys.* **2008**, *104*, 034113.
- (10) Michelon, J.; Hoofman, R. J. Moisture Influence on Porous Low-k Reliability. *IEEE Trans. Device Mater. Reliab.* **2006**, *6*, 169–174.
- (11) Guyer, E. P.; Gantz, J.; Dauskardt, R. H. Aqueous Solution Diffusion in Hydrophobic Nanoporous Thin-Film Glasses. *J. Mater. Res.* **2007**, *22*, 710–718.
- (12) Proost, J.; Baklanov, M.; Maex, K.; Delaey, L. Compensation Effect during Water Desorption from Siloxane-Based Spin-on Dielectric Thin Films. *J. Vac. Sci. Technol., B: Microelectron. Nanometer Struct.—Process., Meas., Phenom.* **2000**, *18*, 303–306.
- (13) Cheng, Y.-L.; Leon, K.-W.; Huang, J.-F.; Chang, W.-Y.; Chang, Y.-M.; Leu, J. Effect of Moisture on Electrical Properties and Reliability of Low Dielectric Constant Materials. *Microelectron. Eng.* **2014**, *114*, 12–16.
- (14) Lam, J. C.; Huang, M. Y.; Tan, H.; Mo, Z.; Mai, Z.; Wong, C. P.; Sun, H.; Shen, Z. Vibrational Spectroscopy of Low-k/Ultra-low-k Dielectric Materials on Patterned Wafers. *J. Vac. Sci. Technol., A* **2011**, *29*, 051513.
- (15) Du, Q.; Freysz, E.; Shen, Y. R. Vibrational Spectra of Water Molecules at Quartz/Water Interfaces. *Phys. Rev. Lett.* **1994**, *72*, 238–241.
- (16) Raghavan, K.; Foster, K.; Berkowitz, M. Comparison of The Structure and Dynamics of Water at The Pt (111) and Pt (100) Interfaces: Molecular Dynamics Study. *Chem. Phys. Lett.* **1991**, *177*, 426–432.
- (17) Rose, D. A.; Benjamin, I. Adsorption of Na⁺ and Cl⁻ at the Charged Water–Platinum Interface. *J. Chem. Phys.* **1993**, *98*, 2283–2290.
- (18) Lenk, R.; Bonzon, M.; Greppin, H. Dynamically Oriented Biological Water as Studied by NMR. *Chem. Phys. Lett.* **1980**, *76*, 175–177.
- (19) Nanjundiah, K.; Hsu, P. Y.; Dhinojwala, A. Understanding Rubber Friction in the Presence of Water Using Sum-Frequency Generation Spectroscopy. *J. Chem. Phys.* **2009**, *130*, 024702–1–7.
- (20) Noguchi, H.; Hiroshi, M.; Tominaga, T.; Gong, J. P.; Osada, Y.; Uosaki, K. Interfacial Water Structure at Polymer Gel/Quartz Interfaces Investigated by Sum Frequency Generation Spectroscopy. *Phys. Chem. Chem. Phys.* **2008**, *10*, 4987–4993.
- (21) Du, Q.; Freysz, E.; Shen, Y. R. Surface Vibrational Spectroscopic Studies of Hydrogen Bonding and Hydrophobicity. *Science* **1994**, *264*, 826–828.
- (22) Baldelli, S.; Schnitzer, C.; Shultz, M. J.; Campbell, D. Sum Frequency Generation Investigation of Glycerol/Water Surfaces. *J. Phys. Chem. B* **1997**, *101*, 4607–4612.
- (23) Che, M.-L.; Teng, J.-Y.; Lai, P.-C.; Leu, J. Moisture Uptake and Dielectric Property of Methylsilsesquioxane/High-Temperature Porogen Hybrids and Porous Low-K Films. *J. Mater. Res.* **2011**, *26*, 2987–2995.
- (24) Li, Q.; Hua, R.; Chou, K. C. Electronic and Conformational Properties of the Conjugated Polymer MEH-PPV at a Buried Film/Solid Interface Investigated by Two-Dimensional IR-Visible Sum Frequency Generation. *J. Phys. Chem. B* **2008**, *112*, 2315–2318.
- (25) Gautam, K. S.; Dhinojwala, A. Molecular Structure of Hydrophobic Alkyl Side Chains at Comb Polymer–Air Interface. *Macromolecules* **2001**, *34*, 1137–1139.
- (26) Su, X.; Cremer, P. S.; Shen, Y. R.; Somorjai, G. A. Pressure Dependence (10^{-10} –700 Torr) of the Vibrational Spectra of Adsorbed CO on Pt (111) Studied by Sum Frequency Generation. *Phys. Rev. Lett.* **1996**, *77*, 3858–3860.
- (27) Chen, Z. Understanding Surfaces and Buried Interfaces of Polymer Materials at The Molecular Level Using Sum Frequency Generation Vibrational Spectroscopy. *Polym. Int.* **2007**, *56*, 577–587.
- (28) Chen, Z. Investigating Buried Polymer Interfaces Using Sum Frequency Generation Vibrational Spectroscopy. *Prog. Polym. Sci.* **2010**, *35*, 1376–1402.
- (29) Chen, Z.; Shen, Y.; Somorjai, G. A. Studies of Polymer Surfaces by Sum Frequency Generation Vibrational Spectroscopy. *Annu. Rev. Phys. Chem.* **2002**, *53*, 437–465.
- (30) Zhang, X.; Chen, Z. Observing Phthalate Leaching from Plasticized Polymer Films at the Molecular Level. *Langmuir* **2014**, *30*, 4933–4944.
- (31) Zhang, C.; Shephard, N. E.; Rhodes, S. M.; Chen, Z. Headgroup Effect on Silane Structures at Buried Polymer/Silane and Polymer/Polymer interfaces and Their Relations to Adhesion. *Langmuir* **2012**, *28*, 6052–6059.
- (32) Zhang, X.; Zhang, C.; Hankett, J. M.; Chen, Z. Molecular Surface Structural Changes of Plasticized PVC Materials after Plasma Treatment. *Langmuir* **2013**, *29*, 4008–4018.
- (33) Zhang, C.; Hankett, J.; Chen, Z. Molecular Level Understanding of Adhesion Mechanisms at the Epoxy/Polymer Interfaces. *ACS Appl. Mater. Interfaces* **2012**, *4*, 3730–3737.
- (34) Zhang, C.; Myers, J. N.; Chen, Z. Elucidation of Molecular Structures at Buried Polymer Interfaces and Biological Interfaces Using Sum Frequency Generation Vibrational Spectroscopy. *Soft Matter* **2013**, *9*, 4738–4761.
- (35) Myers, J. N.; Zhang, C.; Lee, K.-W.; Williamson, J. M.; Chen, Z. Hygrothermal Aging Effects on Buried Molecular Structures at Epoxy Interfaces. *Langmuir* **2014**, *30*, 165–171.

- (36) Trudeau, T. G.; Jena, K. C.; Hore, D. K. Water Structure at Solid Surfaces of Varying Hydrophobicity. *J. Phys. Chem. C* **2009**, *113*, 20002–20008.
- (37) Perry, A.; Neupert, C.; Space, B.; Moore, P. B. Theoretical Modeling of Interface Specific Vibrational Spectroscopy: Methods and Applications to Aqueous Interfaces. *Chem. Rev.* **2006**, *106*, 1234–1258.
- (38) Eisenthal, K. Liquid Interfaces Probed by Second-Harmonic and Sum-Frequency Spectroscopy. *Chem. Rev.* **1996**, *96*, 1343–1360.
- (39) Messmer, M. C.; Conboy, J. C.; Richmond, G. L. Observation of Molecular Ordering at the Liquid–Liquid Interface by Resonant Sum Frequency Generation. *J. Am. Chem. Soc.* **1995**, *117*, 8039–8040.
- (40) Wang, J.; Woodcock, S. E.; Buck, S. M.; Chen, C.; Chen, Z. Different Surface-Restructuring Behaviors of Poly(methacrylate)s Detected by SFG in Water. *J. Am. Chem. Soc.* **2001**, *123*, 9470–9471.
- (41) Ye, H.; Gu, Z.; Gracias, D. H. Kinetics of Ultraviolet and Plasma Surface Modification of Poly(dimethylsiloxane) Probed by Sum Frequency Vibrational Spectroscopy. *Langmuir* **2006**, *22*, 1863–1868.
- (42) Hankett, J. M.; Lu, X. L.; Liu, Y. W.; Seeley, E.; Chen, Z. Interfacial Molecular Restructuring of Plasticized Polymers in Water. *Phys. Chem. Chem. Phys.* **2014**, *16*, 20097–20106.
- (43) York, R. L.; Li, Y.; Holinga, G. J.; Somorjai, G. A. Sum Frequency Generation Vibrational Spectra: The Influence of Experimental Geometry for An Absorptive Medium or Media. *J. Phys. Chem. A* **2009**, *113*, 2768–2774.
- (44) Proost, J.; Kondoh, E.; Vereecke, G.; Heyns, M.; Maex, K. Critical Role of Degassing for Hot Aluminum Filling. *J. Vac. Sci. Technol., B: Microelectron. Nanometer Struct.—Process, Meas., Phenom.* **1998**, *16*, 2091–2098.
- (45) Liu, M.; Wu, P.; Ding, Y.; Chen, G.; Li, S. Two-Dimensional (2D) ATR-FTIR Spectroscopic Study on Water Diffusion in Cured Epoxy Resins. *Macromolecules* **2002**, *35*, 5500–5507.
- (46) Zhang, C.; Chen, Z. Probing Molecular Structures of Poly(dimethylsiloxane) at Buried Interfaces *in situ*. *J. Phys. Chem. C* **2013**, *117*, 3903–3914.
- (47) Shen, Y. R.; Ostroverkhov, V. Sum-Frequency Vibrational Spectroscopy on Water Interfaces: Polar Orientation of Water Molecules at Interfaces. *Chem. Rev.* **2006**, *106*, 1140–1154.
- (48) Ostroverkhov, V.; Waychunas, G. A.; Shen, Y. Vibrational Spectra of Water at Water/A-Quartz (0001) Interface. *Chem. Phys. Lett.* **2004**, *386*, 144–148.